Efficient production of few-layer graphene by shear exfoliation of graphite in an aqueous liquid

Mingyun Guo[1], Jian Cui[1], Guangfa Zhang[1], Shuai Zhao[1], Ailin Gao[1], and Yehai Yan[1]

[1]Qingdao University of Science and Technology

September 24, 2020

Abstract

A water-soluble polymer stabilizer (VIB-co-VI-co-Py, Figure 1) assisted liquid-phase exfoliation (LPE), implemented by high-shear mixing rather than currently more often used bath/probe sonication, was developed as a new method for efficient production of few-layer graphene (FLG) in aqueous liquid. With help of VIB-co-VI-co-Py, stable aqueous dispersion of FLG forms in-situ with 90% of dispersed flakes of fewer than five layers and production rate up to 0.86 g h-1 by 5.0 L of aqueous liquid, representing the highest production rate per volume (0.17 g L-1 h-1) reported hitherto for LPE with the liquid volume no less than 5.0 L. The scale-up shear-exfoliated FLG exhibits high quality and excellent redispersibility in water, thus paving the way for a wide range of applications. As typical application demonstrations, the FLG-based flexible conductive films and polymer composite hydrogels were prepared and evaluated. The results show that the VIB-co-VI-co-Py exfoliated FLG performs well therein.

KEYWORDS

Few-layer graphene, Shear exfoliation, Aqueous liquid, Polymer stabilizer, Colloidal dispersion

INTRODUCTION

On basis of two-dimensional nature, single atom thickness, and unprecedented properties, graphene gains the honor "wonder material" with great potential for various applications from composites to electronics. Although prominent progress has been made in the last two decades, graphene still faces some challenges for advancing its practical applications. A major one is to massively acquire high-quality but low-cost graphene in a green and efficient manner. For that matter, the bottom-up strategy that resorts to chemical synthesis to produce graphene is not under consideration for its production-scale limitation and high-cost at the current stage of technique development.[1,2] By contrast, the top-down one turns to mechanical exfoliation of graphite to get graphene and/or FLG, exhibiting a high feasibility for cost-efficient massive production.[3] Of the developed methods under top-down strategy, LPE arouses a particular interest.[4,5] Besides possessing the general advantages of top-down strategy, LPE renders as-exfoliated FLG directly forming a stable uniform dispersion, greatly facilitating integration of FLG into various practical systems through diverse dispersion-based processes. LPE has accordingly become one of the most extensively explored methods for producing graphene.

Any energy source capable of providing an energy density high enough to overcome the cleavage energy of graphite (35-61 meV/atom)[6] is competent for FLG exfoliation. Under this guideline, the probe/bath sonicators that can afford thousands of W L^{-1} of energy densities have been extensively employed for exfoliation of graphite.[5,7] It is a pity, however, that the sonication-driven exfoliation method is not practicable for scale production. To achieve >1.0 mg mL^{-1} of as-exfoliated FLG dispersion, one has to significantly extend the

1

sonication time (as long as hundreds of hours), which induces not only a very low production rate (down to 3.1 mg h^{-1}) but a remarkable amount of defects built upon the graphene basal plane.[3-5,8-10] What's more, the exfoliation process is strongly influenced by many other factors, such as vessel geometry, vessel position in bath, water level of bath, and energy output of sonicator that usually deviates from the rated value. This makes poor reproducibility become another shortcoming for scale-up of sonication-driven LPE. Against this background, a fluid dynamics-based LPE performed by a vortex fluidic device, jet cavitation device, rotor-stator mixer, or even kitchen blender emerges recently.[7,11-13] In such a process, graphite moves fast with liquid and can be repeatedly exfoliated at different positions of the vessel. Relative to sonication exfoliation, this exfoliation way has a higher possibility to get basal defect-free FLG because the energy density deposited on graphene basal plane is much lower than that exerted by sonicator,[7] thus making it a promisingly efficient process for mass production of high-quality FLG. Of all the hired devices for driving fluid dynamics, the rotor-stator mixer is of particular concern.[7,14-16] As an easily available high-shear mixer, it has been industrially employed for many applications, such as dispersing nanoparticles in liquids. When the shear rate () is higher than $10^4 s^{-1}$, it was shown to be also applicable for exfoliation of graphite into FLG.[7] With the optimized processing parameters, the FLG production rate reaches 5.3 g h^{-1}, far higher than any reported work, and may be further improved to 100 g h^{-1} by scaling up the liquid volume to 10 m^3. Accordingly, the rotor-stator mixer-mediated shear exfoliation is regarded as, even if not exclusive, one of the most industrially feasible methods for mass production of defect-free FLG.[7]

Considering that water is a low-cost and eco-friendly solvent and aqueous FLG dispersion has many important applications, such as water-soluble polymer composites and conductive coatings,[17,18] it is highly desirable for FLG exfoliation to be performed in aqueous liquid. However, the big surface energy mismatch is a huge hurdle to exfoliate and disperse FLG in water. A forthright solution is to utilize a water-soluble stabilizer. By far, various surfactants,[19-21] aromatic compounds,[22-24] polymers,[25-36] and even inorganic nanoparticles[37-39] have been explored as stabilizers. Among them, polymer stabilizers attract specific attention. Compared with small molecules, polymers having longer chains may provide more active sites to solvate nano substance and higher steric volume to push nano substance away from each other for stabilization. In fact, many research efforts have revealed that polymers are assuredly more efficient than small molecules in achieving higher FLG concentrations.[21-23] Additionally, it is different from most of small molecules, which often has adverse effects on the performances of FLG-derived products, that polymers act concurrently as a useful component in subsequent applications of aqueous FLG dispersion, contributing some functionalities, such as chemical sensing,[25] enzyme immobilization,[30] and DNA recognition.[35] These merits promote polymers to come into the most prevalent stabilizers for FLG exfoliation.

As an effort to advance the practical applications of graphene, a polymer stabilizer-assisted, rotor-stator mixer-mediated shear exfoliation method was developed for efficient production of high-quality FLG in aqueous liquid. For this, VIB-*co*-VI-*co*-Py (Figure 1), a water-soluble vinylimidazole-based polymer,[25] was selected as stabilizer. It has been previously proven a successful stabilizer in producing FLG by sonication-driven aqueous phase exfoliation of graphite.[40] Another reason for selection of VIB-*co*-VI-*co*-Py is due to its imidazole rings, which have bioactivity and pharmaceutical activity and exist in many biomolecules and drugs.[41] It is reasonably presumed that the VIB-*co*-VI-*co*-Py exfoliated FLG is applicable to the biomedical uses. In this work, VIB-*co*-VI-*co*-Py was demonstrated also successful in FLG production by shear exfoliation of graphite. The rotor-stator mixer-mediated FLG exfoliation was executed in aqueous liquid and discussed from aspects of FLG concentration, production yield, and dispersion stability. Then the dispersed flakes were carefully characterized. It was found that the as-exfoliated FLG forms a stable colloidal dispersion with the production rate up to 0.86 g h^{-1} by 5.0 L of aqueous liquid. To our knowledge, this is the highest production rate per volume (0.17 g L^{-1} h^{-1}) hitherto for LPE with the liquid volume higher than 5.0 L. In addition, the shear-exfoliated FLG shows a high exfoliation level, high quality, and excellent redispersibility in water. Finally, the as-obtained FLG was demonstrated to perform well in two typical applications, *i.e.* flexible conductive films and polymer composite hydrogels.
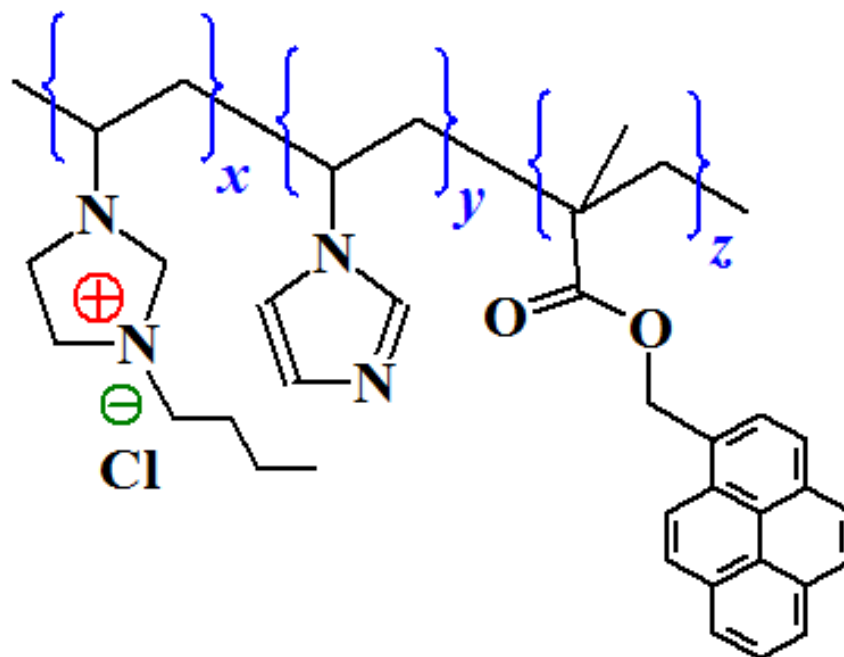
2

FIGURE 1 Chemical structure of VIB-*co*-VI-*co*-Py ($x : y : z = 47 : 50 : 3$).

EXPERIMENTAL

2.1 Materials

Graphite with particle size quoted as +100 mesh (Product number 332461) was supplied by Aldrich. VIB-*co*-VI-*co*-Py with VIB/VI/Py = 47/50/3 (mol/mol) was synthesized according to a reported method.[40] Dimethyl acrylamide (DMAA), methylene bisacrylamide (MBA), tetramethyl ethylenediamine (TEMEDA), and ammonium persulfate (APS) were purchased from Aladdin. In all relative experiments, the ultrapure water (18.25 MΩ cm) was used.

Exfoliation of graphite into FLG

Into a 250 mL beaker, 150 mL of aqueous VIB-*co*-VI-*co*-Py solution and desired amount of graphite were added in turn. Subsequently, a high-shear mixing process was performed by a Silverson L5M mixer with a 4-blade rotor (32 mm diameter) and a square-hole screen (96 holes, each 2×2 mm^2) separated from each other by a 135 μm gap. After mixing for a preset time and sitting for 6 h, the mixture was experienced 90 min of centrifugation at 2,000 rpm, and 2/3 of supernatant was gently sucked out. Thus collected dispersion was directly used for determining the concentration of FLG and evaluating its stability. For other studies, the excess VIB-*co*-VI-*co*-Py was eliminated by repetitiously filtering the dispersion through a 0.2 μm hydrophilic membrane and redispersing filter-cake in fresh water until no VIB-*co*-VI-*co*-Py was monitored in filtrate by UV spectroscopy. The resultant filter-cake was vacuum-dried for 10 h at 60 °C and named as**FLG-P** hybrid.

3

Synthesis of hydrogels

To synthesize the poly(N ,N -dimethyl acrylamide)/FLG (PDMAA/FLG) hydrogel, **FLG-P** hybrid (1.0 wt% of DMAA) was first dispersed in DMAA to yield a uniform dispersion by 5 min sonication. Then, 1.0 mL of such dispersion was injected into a 25 mL beaker containing 3.8 mL of aqueous solution of MBA (0.1 wt% of DMAA) and 7.7 μL of TEMEDA (0.6 wt% of DMAA), followed by 30 s sonication. After being kept in an ice-water bath and bubbled with high-purity N_2 for 15 min, 0.2 mL of aqueous solution of APS (0.6 wt% of DMAA) was introduced, bubbled for another 5 min, and transferred into a plastic syringe (2 mL) or a home-made glass mold ($50 \times 50 \times 1$ mm^3). Finally, the syringe or glass mold was sealed and kept at 35 °C for 24 h to complete the hydrogel synthesis. Following the same procedures, the PDMAA hydrogel was also synthesized.

Characterization

UV-VIS and Raman spectra were collected respectively from TU-1901PC and Renishaw inVia micro-Raman (with a 532 nm laser) spectrometers. Both dynamic light scattering (DLS) and zeta potential tests were conducted on a Zetasizer Nano-ZS system (Malvern) equipped with a 633 nm laser. Thermogravimetric analyses (TGA) were performed by TA-Instruments Q500 in N_2 at the heating rate of 10 °C min^{-1}. Tapping-mode atomic force microscopy (AFM) and transmission electron microscopy (TEM) were done using Bruker Multimode 8 and JEOL JEM-2100 microscopes, respectively. Electrical conductivities of FLG films were evaluated on a Model RTS-8 multimeter using the four-probe method, whereas those of hydrogels were measured on a Keithley 2636B multimeter connected with a test fixture using the two-probe method.[42] For mechanical testing, the hydrogel samples were cut into 50 mm × 10 mm × 1 mm specimens and assessed by Zwick/Roell Z005 at a tensile speed of 30 mm min^{-1}.

RESULTS AND DISCUSSION

FLG exfoliation was performed by high-shear mixing of graphite in an aqueous solution of VIB-co -VI-co -Py. In this process, the mixer rotor speed was optimized and fixed at 4,500 rpm (Supporting Information (SI): Section I), corresponding to = 5.6×10^4 s^{-1} that is safely beyond the minimum required for FLG exfoliation ($_{\min}$ [?] 10^4 s^{-1}).[7] As to centrifugation, an important procedure for collection of FLG, it was fixed at 2,000 rpm/90 min. Previous studies have shown that 500-2,000 rpm/90 min is enough for removing most of unwanted thick particles, and further increasing centrifugation speed induces basal defect-rich FLG sheets concentrated in the supernatant.[21,43] Hence, this work on FLG exfoliation centers only on the parameters of VIB-co -VI-co -Py concentration ($C_{\mathbf{P}}$), initial graphite concentration ($C_{\mathbf{G,i}}$), and mixing time ($t_{\mathbf{M}}$).

Using FLG concentration ($C_{\mathbf{G}}$) as an evaluation index, optimization of $C_{\mathbf{P}}$ was performed at the constant $C_{\mathbf{G,i}}$ of 3.0 mg mL^{-1} and $t_{\mathbf{M}}$ of 20 min. After the shear mixing and centrifugation separation, a homogeneous colloidal dispersion is obtained regardless of variation of $C_{\mathbf{P}}$ (inset of Figure 2a). In the absence of VIB-co -VI-co -Py, however, the graphitic particles completely settle in water. For fast determination of $C_{\mathbf{G}}$, a well-developed spectroscopic method [8] was adopted with an absorption coefficient of a $_{\mathrm{G,660}}$ = 2,751 mL mg^{-1}m^{-1} (SI: Section II). Figure 2a depicts the $C_{\mathbf{G}}$ dependence on $C_{\mathbf{P}}$. It is shown that $C_{\mathbf{G}}$ increases with increasing $C_{\mathbf{P}}$ and reaches the maximum of 6.3 μg mL^{-1} at $C_{\mathbf{P}}$ = 2.0 mg mL^{-1}. Further increase of $C_{\mathbf{P}}$ causes the leveling off of $C_{\mathbf{G}}$. Similar dependence also takes place at $C_{\mathbf{G,i}}$ = 25, 50, and 80 mg mL^{-1}, where $C_{\mathbf{G}}$ reach the maxima of 0.082, 0.181, and 0.239 mg mL^{-1}respectively at $C_{\mathbf{P}}$ = 1.75, 2.0, and 2.0 mg mL^{-1} (Figure 2b). The critical $C_{\mathbf{P}}$ of ~2.0 mg mL^{-1} is obviously higher than 0.6 mg mL^{-1} that was optimized for VIB-co -VI-co -Py in the sonication-driven FLG exfoliation.[25] Besides, in sonication exfoliation, $C_{\mathbf{G}}$ begins to decrease when $C_{\mathbf{P}}$ exceeds 0.6 mg mL^{-1}. The reason behind these disparities may be due to the different morphology and dimension of VIB-co -VI-co -Py against sonication and shear mixing. As was previously noticed, micelles are formed in aqueous solutions of VIB-co -VI-co -Py and their average sizes (26.3-465.2 nm)
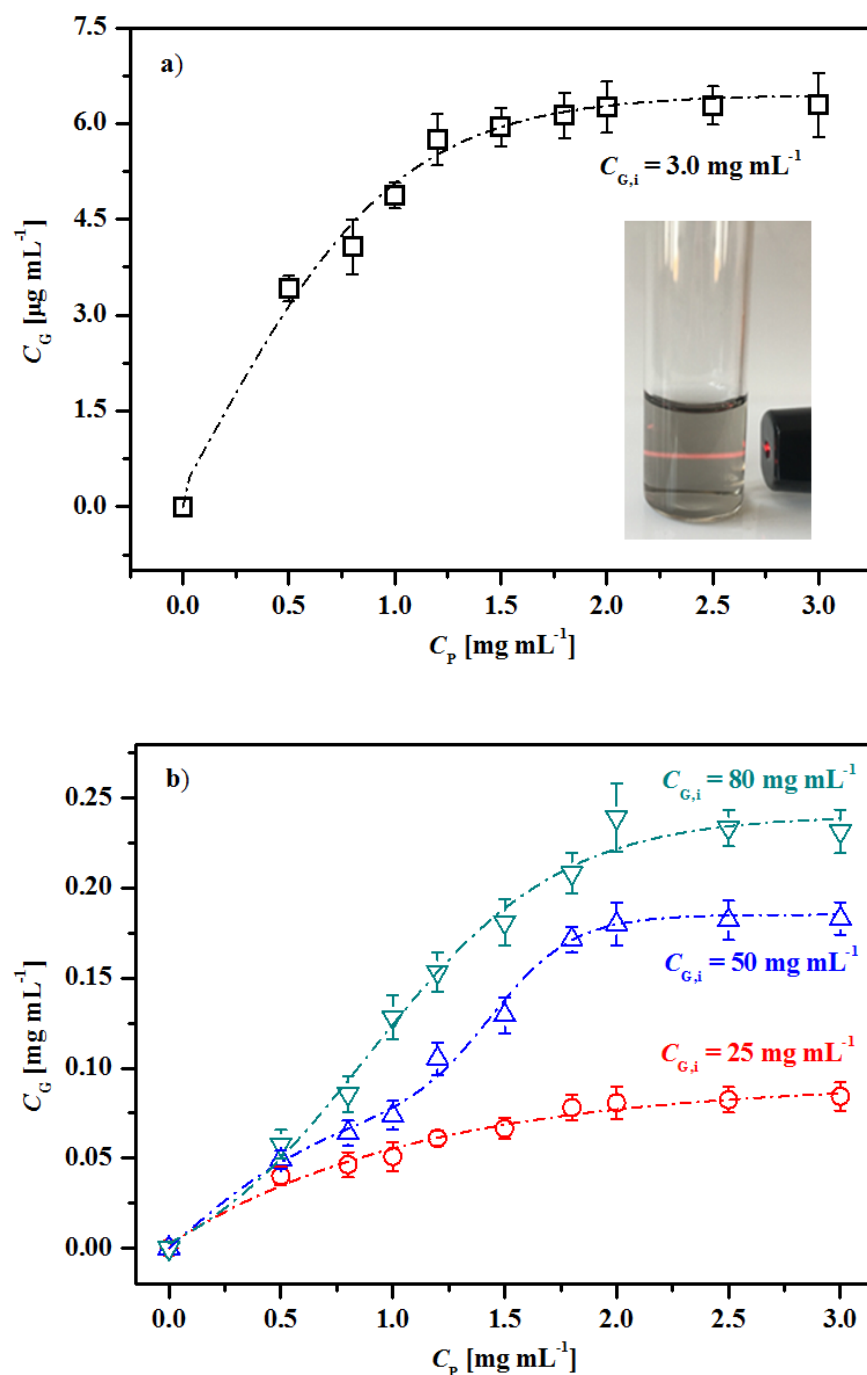
4

FIGURE 2 Dependence of C_G on C_P with $C_{G,i}$ keeping constant at a) 3.0 mg mL^{-1} and b) 25, 50, and 80 mg mL^{-1}. Inset: photograph of an aqueous FLG dispersion produced with $C_P = 2.0$ mg mL^{-1} and $C_{G,i} = 3.0$ mg mL^{-1} (therein the Tyndall effect is shown).

increase with increasing C_P (0.1-2.0 mg mL^{-1}).[25] It was well documented that micelles, especially the large-sized ones, cannot fit into adjacent nanoparticles.[44] As a consequence, the osmotic pressure of micelles around nanoparticles generates a strong depletion attraction, causing aggregation of nanoparticles and thus decrease

of the dispersion concentration. In the sonication process, the cavitation effect makes it possible that no micelles or only small ones are formed in aqueous solutions until $C_\mathbf{P}$ is higher than 0.6 mg mL^{-1}. Under the shear-mixing condition, however, the critical $C_\mathbf{P}$ for formation of micelles with sizes large enough to create effective depletion attraction seems to be improved to higher than 3.0 mg mL^{-1} (maximal $C_\mathbf{P}$ examined in this work), owing to serious micelle breakage brought by the combined high shear, cavitation, and collision effects.[3] Higher $C_\mathbf{P}$ but absence of large-sized micelles is helpful to facilitate exfoliation, dispersion, and stabilization of FLG, particularly in the cases of higher $C_\mathbf{G,i}$. Almost constant $C_\mathbf{G}$ observed within 2.0-3.0 mg mL^{-1} of $C_\mathbf{P}$ is attributed to adsorption of polymers on the graphitic particle surface already reaching saturation and more polymers having little influence on dispersing FLG.

The aqueous solution of $C_\mathbf{P}$ = 2.0 mg mL^{-1} was then selected as liquid medium to study the influence of $C_\mathbf{G,i}$ on $C_\mathbf{G}$. As shown in Figure 3a, $C_\mathbf{G}$ increases monotonously with $C_\mathbf{G,i}$ in the detected range of 3.0-80 mg mL^{-1}. Such an increase trend is different from that of sonication exfoliation, where $C_\mathbf{G}$ usually tends to decrease beyond a certain $C_\mathbf{G,i}$ (10-60 mg mL^{-1}) whose specific value depends on selection of sonication mode and water-soluble stabilizer.[25,30,45] It is well established that sound cavitation is the primary driving force for sonication-assisted FLG exfoliation.[3] Too high $C_\mathbf{G,i}$ may block the sound propagation and thus weaken the exfoliation efficiency. In the case of shear exfoliation, however, shearing force dominantly responsible for FLG exfoliation is long-range relative to sound wave, and its transmission is little affected by $C_\mathbf{G,i}$ (at least within the currently examined $C_\mathbf{G,i}$ range). Figure 3a also reveals that $C_\mathbf{G}$ relates with $C_\mathbf{G,i}$ in an empirical form of $C_\mathbf{G} [?] C_\mathbf{G,i}{}^{1.17}$. This power-law correlation was as well observed in sonication exfoliation with the exponents falling in 0.5-0.8.[30,46,47] Much higher value achieved here (1.17) reflects an obviously faster increase of $C_\mathbf{G}$ with $C_\mathbf{G,i}$, indicating high-shear mixing more efficient in FLG exfoliation than sonication. What should be pointed out is that the exponent of 1.17 is realized by merely 20 min of $t_\mathbf{M}$ and, meanwhile, $C_\mathbf{G}$ is up to 0.24 mg mL^{-1}. In stark contrast, it usually requires several or even tens of hours to get such a comparable $C_\mathbf{G}$ by sonication exfoliation.[21,48] Despite monotonous increase of $C_\mathbf{G}$ with $C_\mathbf{G,i}$, a parabolic-like dependence of production yield ($C_\mathbf{G}/C_\mathbf{G,i}$) on $C_\mathbf{G,i}$ is noted with $C_\mathbf{G}/C_\mathbf{G,i}$ reaching the maximum of 0.38% at $C_\mathbf{G,i}$ = 50 mg mL^{-1} (Figure 3b), compared with a quasi-linear decline of $C_\mathbf{G}/C_\mathbf{G,i}$ with increasing $C_\mathbf{G,i}$ in sonication exfoliation.[25,30,46] This again demonstrates that the shear exfoliation is superior to sonication exfoliation from the viewpoint of capacity for improving $C_\mathbf{G}/C_\mathbf{G,i}$.
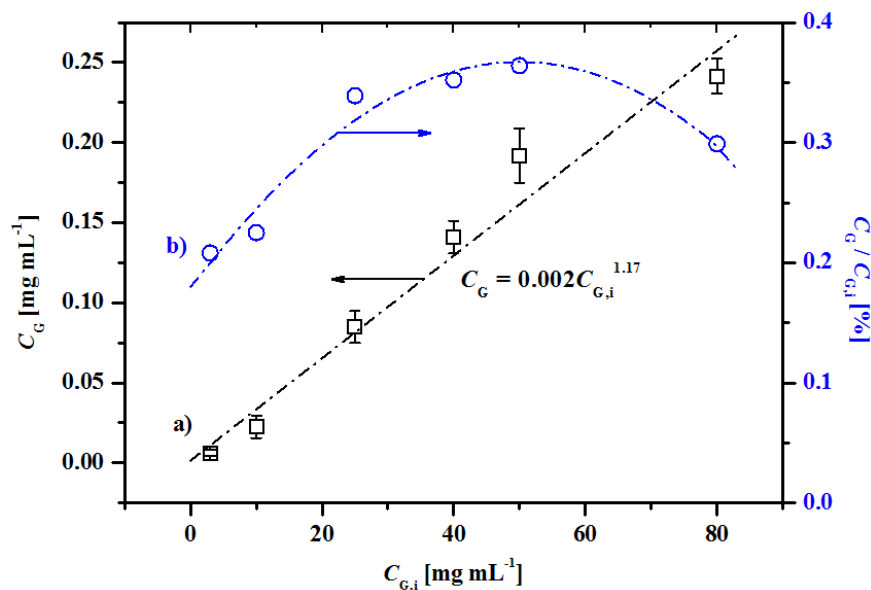

FIGURE 3 Dependence of a) $C_\mathbf{G}$ and b) $C_\mathbf{G}/C_\mathbf{G,i}$ on $C_\mathbf{G,i}$.

The effect of t_M on FLG exfoliation was explored by fixing $C_P = 2.0$ mg mL^{-1} and $C_{G,i} = 50$ mg mL^{-1}. As observed from Figure 4a, C_G (thus $C_G/C_{G,i}$) increases steadily from 0.092 mg mL^{-1} at $t_M = 5$ min to 0.33 mg mL^{-1} at $t_M = 80$ min, showing an empirical correlation of C_G [?]$t_M^{0.57}$. The exponents close to 0.5-0.7 were also noticed in sonication exfoliation and other instances of shear exfoliation and proposed to be process-independent, reflecting a more fundamental behavior.[7,9,49] Above 80 min of t_M, C_G tends to saturate. On the other hand, extension of t_M decreases the lateral size of FLG. With t_M extended from 5 to 20, 80, and 180 min, the average lateral size of FLG determined by DLS decreases from 829 ± 218 to 713 ± 180, 583 ± 115, and 304 ± 97 nm (Figure 4b). Larger lateral size thus higher aspect ratio is desired for many applications of FLG, such as polymer composites. Upon systematic consideration of FLG size, exfoliation efficiency, and $C_G/C_{G,i}$, the parameter combination of $C_P = 2.0$ mg mL^{-1}, $C_{G,i} = 50$ mg mL^{-1}, and $t_M = 80$ min is preferred for subsequent scale-up production of FLG.
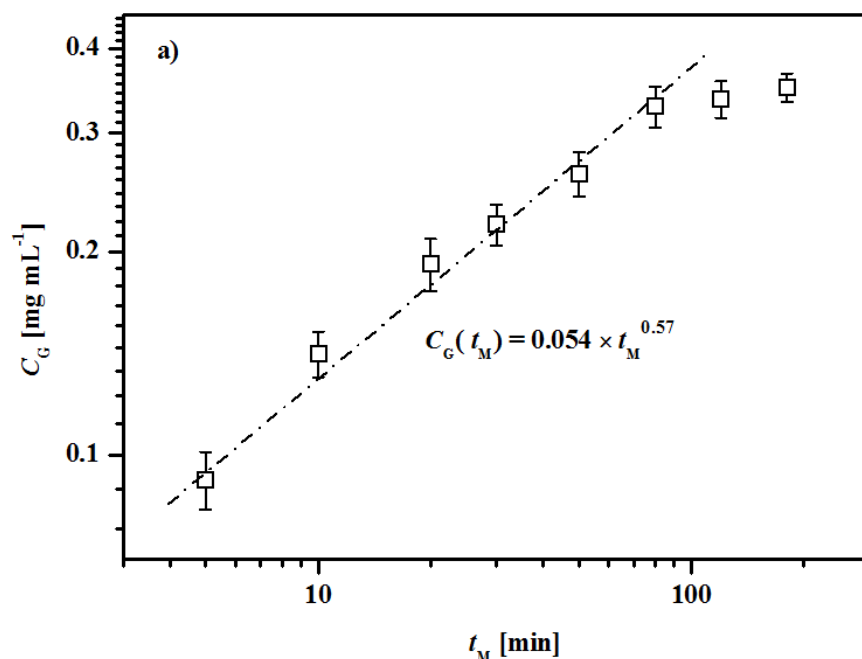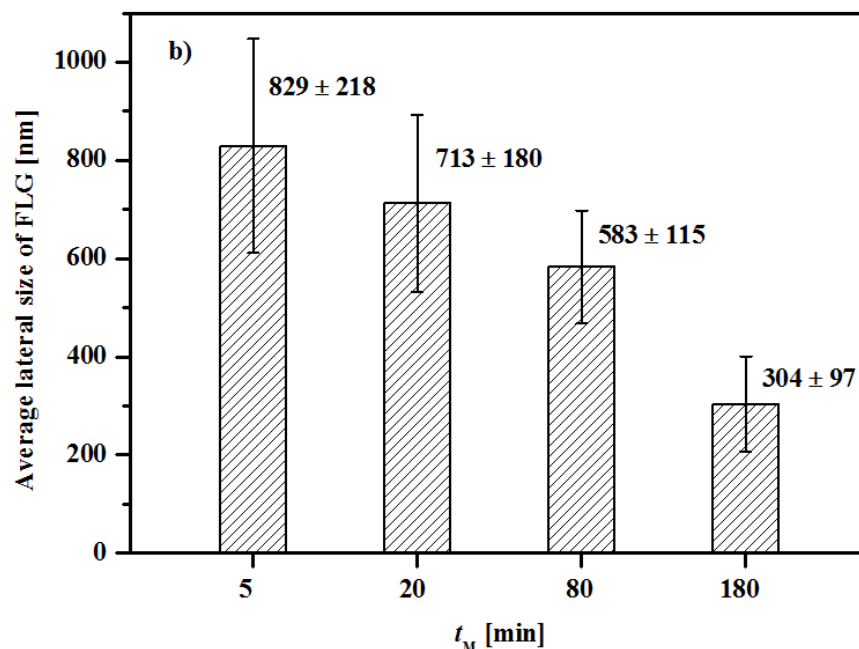
FIGURE 4 Dependence of a) C_G and b) FLG size (identified by DLS) on t_M .

The scale-up trials were conducted in home-made Teflon beakers containing 0.5-5.0 L of aqueous liquids. Inner diameter of each beaker was designed to achieve the desirable liquid volume (V) when the liquid height was set equal to the beaker diameter for elimination of the possible geometry effect on shear mixing.[50] These trials produced as high as 1.15 g of FLG per batch with the production rate (P_R) up to 0.86 g h^{-1} (Figure 5). The fitting correlation of $P_R = 0.23 \times V^{0.81}$ allows one to reasonably predict that it may realize ~10 g h^{-1} of P_R upon scale-up of $V = 100$ L. To facilitate comparison among different studies, the production rate per liquid volume (P_R/V) was adopted as a new criterion for evaluation of FLG production. A detailed literature survey (SI: Section III) shows that 0.17 g L^{-1} h^{-1} of P_R/V reached here by $V = 5.0$ L is superior to most of those (1.2×10^{-4}-9.78 g L^{-1} h^{-1}) achieved by sonication- and shear-exfoliation with aqueous liquids and is the highest (1.6×10^{-3}-8.3 x 10^{-2} g L^{-1} h^{-1}) for V [?] 5.0 L. High efficiency of this FLG production method, *i.e.* VIB-*co* -VI-*co* -Py assisted shear exfoliation, is thus demonstrated.
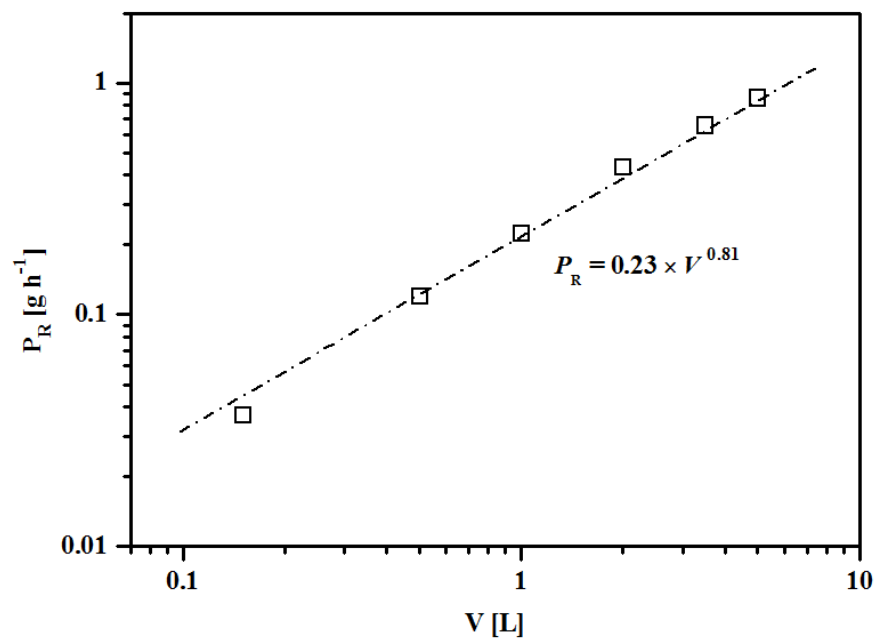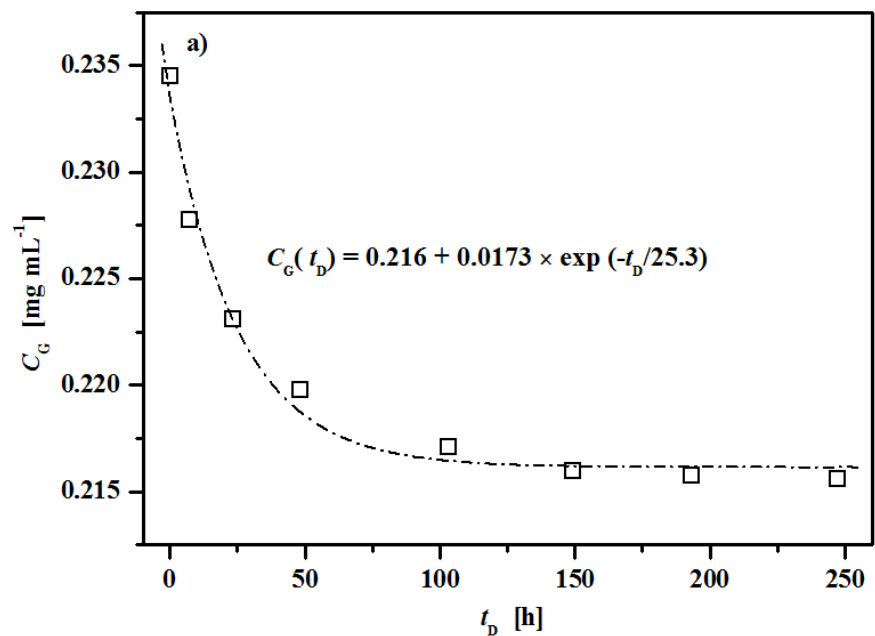
8

FIGURE 5 Dependence of P_R on V .

Stability of the scalably produced dispersion with $V = 5.0$ L was evaluated by monitoring variation of C_G with the deposition time (t_D). As given in Figure 6a, C_G shows an exponential decay with extending t_D that can be quantified as C_G $(t_D$) $= C_s + (C_0 - C_s)e^{-\tau/\tau}$ (C_s – stable phase
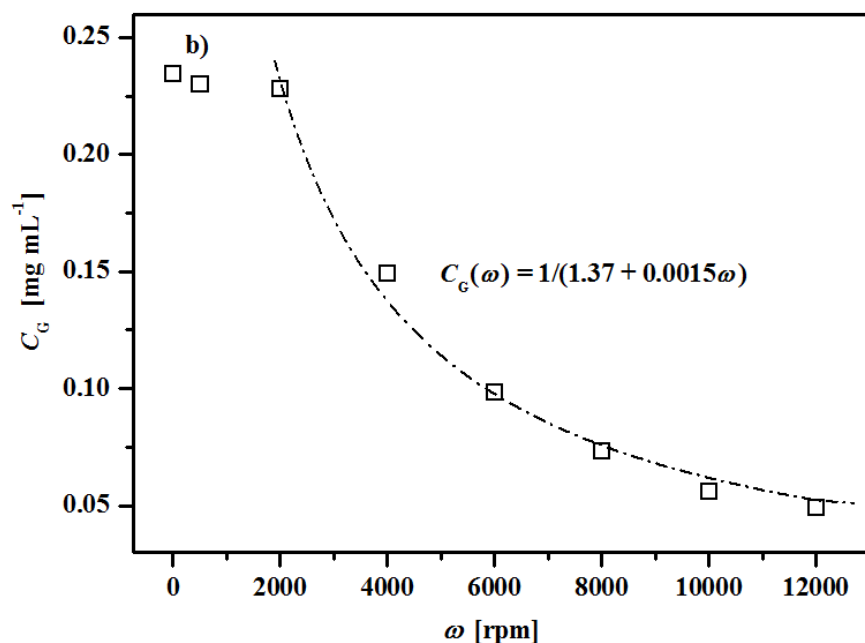

9

FIGURE 6 Dependence of C_G on a) t_D and b) ω.

concentration, C_0 – initial concentration of dispersion, and τ – constant of t_D). On the basis of monitoring data, C_s and τ are determined respectively to be 0.22 mg mL^{-1} and 25 h, indicating 92% of FLG sheets still remaining in the dispersion even after 250 h of deposition. Such good stability is thought to result mainly from electrostatic repulsion of VIB-*co*-VI-*co*-Py adsorbed on the FLG surface. Zeta potential (ξ), a parameter usually used for evaluation of repulsion, is measured as 37.8 mV for the FLG dispersion, while $|\xi| > 30$ mV is a widely accepted cut-off range for colloidal stability.[51] The dependence of C_G on centrifugation speed (ω) was also evaluated (Figure 6b). After 30 min centrifugation, the dispersion shows a negligible decrease of C_G at ω [?] 2,000 rpm. It is because the dispersion has already experienced a centrifugation of 2,000 rpm/90 min in its production process. Over 2,000 rpm, C_G decreases sharply from 0.228 to 0.073 and 0.049 mg mL^{-1} at 8,000 and 12,000 rpm, respectively, exhibiting an empirical scaling of C_G [?] ω^{-1}. Despite undesirable decrease of C_G, a positive phenomenon is observed. That is, the content of single-layer graphene improves to 33% and 76% respectively in 8,000 rpm- and 12,000 rpm-centrifuged supernatants, compared with 11% in 2,000 rpm-centrifuged one (SI: Section IV). This offers an alternative method to produce the single-layer graphene.

FLG-P hybrid prepared from scalably produced dispersion, hereafter named as **FLG-P-80** hybrid, displays an unusual ability of being invertibly dried and re-dispersed in pure water (by 5 min sonication) for many rounds. The thus re-obtained dispersion has a maximal C_G of 3.87 mg mL^{-1}, still reaching 3.23 mg mL^{-1} even after being deposited for 240 h. Such re-dispersing ability, which is believed to be contributed by VIB-*co*-VI-*co*-Py adsorbed on the FLG surface, is absent from reduced graphene oxide (rGO) and most of surfactant-exfoliated FLG, highly facilitating the storage, delivery, and applications of FLG. The content of VIB-*co*-VI-*co*-Py in **FLG-P-80** hybrid is determined to be 6.8 wt% by TGA (SI: Section V).

Taking the aqueous dispersion of **FLG-P-80** hybrid as a typical sample, AFM was carried out to examine the exfoliation state of FLG. Figure 7a presents a typical AFM height image with a cross-section analysis. The analytical results on 107 different flake-like structures reveal that the thickness is mostly within 1.1-2.8 nm (Figure 7b-i). In light of the AFM thickness of pristine graphene usually within 0.6-0.9 nm,[52,53] the determined thickness of 1.1-2.8 nm signifies that 90% of detected flakes are single- (9%), double- (17%), or few-layer (3- to 5-layer, 64%) graphene sheets adsorbed with VIB-*co*-VI-*co*-Py thin layers. Furthermore,

10

the average lateral size of flakes is determined to be 533 ± 102 nm (Figure 7b-ii), in good agreement with the DLS value of 583 ± 115 nm. Within instrumental resolution, no defects like holes were observed on the basal planes, indicative of high quality of the FLG sheets.
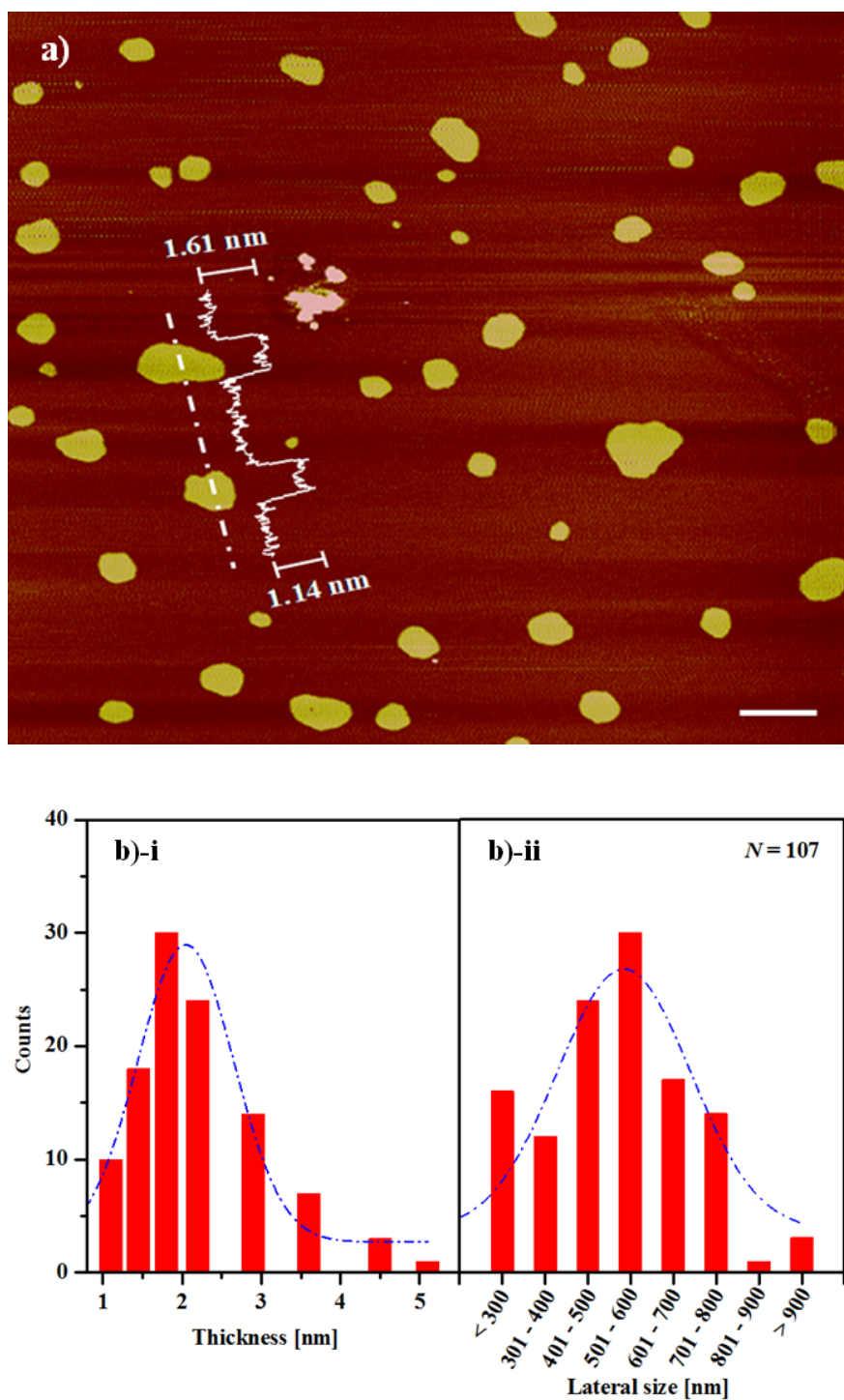

FIGURE 7 a) AFM height image (scale bar - 1.0 μm) and b) distributions of (i) thickness and (ii) lateral

size of**FLG-P-80** hybrid.

The above AFM analyses get support from TEM studies. Once again, numerous flakes with smooth surface and well-resolved edges are observed (Figure 8a and SI: Section VI). The folded structure arrowed in Figure 8a, reflecting the characteristics that a 2D graphene sheet tends to fold to obtain the thermodynamic stability through static microscopic crumpling,[54] is
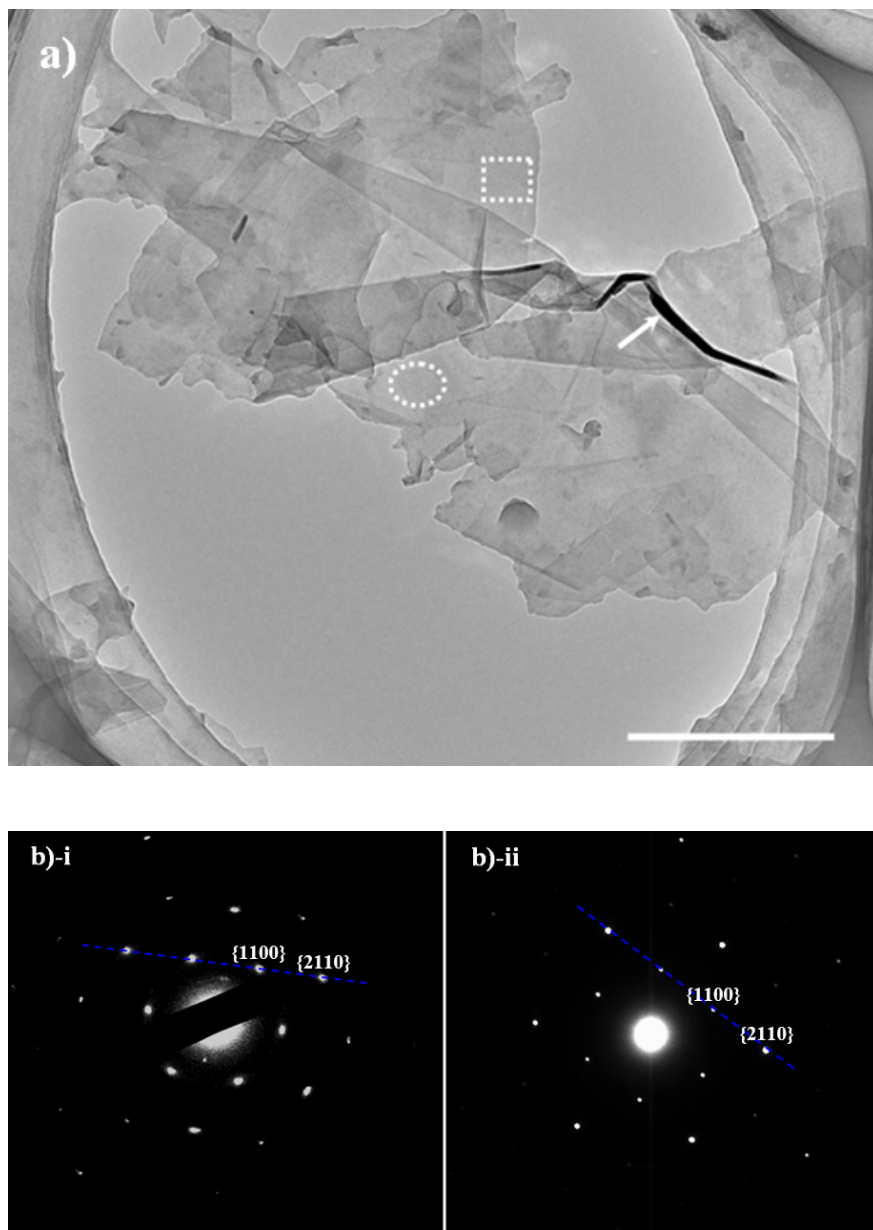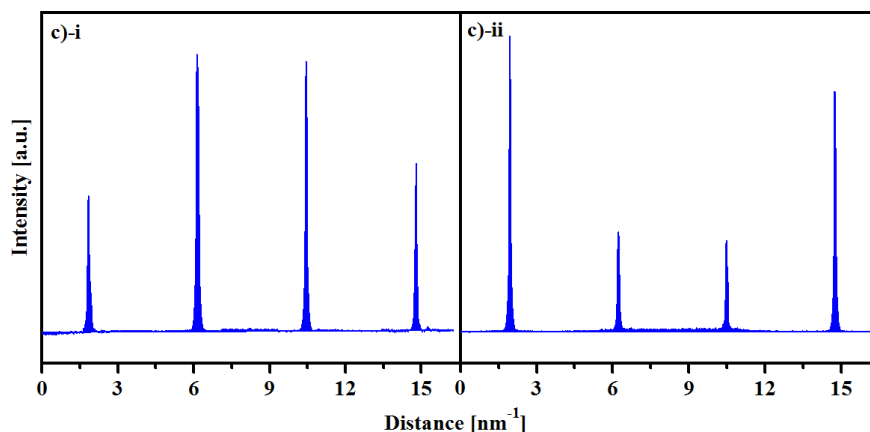
FIGURE 8 a) TEM image of **FLG-P-80** hybrid (scale bar - 500 nm), b) SAED patterns of (i) circled and (ii) framed flakes in a), and c) intensity analyses along the dashed lines in b).

frequently seen in our FLG sample. It seems that the adsorbed pyrenyl-containing polymers promote the folding as a result of π-π interaction with the other graphene surface. The selected area electron diffraction (SAED) patterns exhibit a diagnostic six-fold symmetry expected for graphene (Figure 8b), meaning that shear mixing induces few lattice defects in the graphene framework.[55] Further, the SAED pattern can be used for determination of the layer number of flake. As previously proposed, the flake with stronger {1100} diffraction spot than {2110} one is single-layer graphene, while one with weaker {1100} spot is FLG.[8] According to this proposition, the circled flake (Figure 8a) that has an intensity ratio of {1100} to {2110} ($I_{\{1100\}}/I_{\{2110\}}$) of 1.6 (Figure 8c-i) is recognized as a single-layer graphene; the framed flake (Figure 8a) having an $I_{\{1100\}}/I_{\{2110\}}$ value of 0.5 (Figure 8c-ii) is identified as a FLG.

The quality (defect content) of **FLG-P-80** hybrid was assessed by Raman spectroscopy. For comparison, graphite was also evaluated in parallel. Each spectrum given in Figure 9 is averaged from five spectra collected from different locations on a 1.0 cm diameter sample. The defect content is defined as the D-to-G band intensity ratio, denoted generally as I_D/I_G . It is noticed that I_D/I_G of **FLG-P-80** increases to 0.30 from 0.05 for graphite, suggesting some new defects having been introduced. Even so, this value accords with that of stabilizer- assisted sonication- and other shear-exfoliated FLG (I_D/I_G = 0.10-0.80) [8,12,15,25,43] and is much lower than that of rGO reduced by hydrazine (I_D/I_G = 1.44)[56] or sodium borohydride (I_D/I_G = 1.08).[57] It is well-known that rGO includes a high content of basal and edge defects resulting from severe oxidation treatment. A small increase of I_D/I_G of **FLG-P-80** thus predicts that the shear-exfoliation process adopted here produces very few basal defects and merely moderate quantity of edge ones. Besides being confirmed by AFM and TEM (Figures 7a and 8), this prediction is endorsed by the Raman study on **FLG-P-20** hybrid that was prepared from the dispersion produced at t_M = 20 min. Compared with **FLG-P-80** hybrid, a lower defect content of 0.14 is noticed in the **FLG-P-20** hybrid, exactly corresponding with the larger lateral size of FLG in its master dispersion (Figure 4b) and thus less edges per unit mass. The 2D-band is another Raman spectral feature, which exhibits the different shapes between graphite and **FLG-P** hybrids. A sharp peak (2680 cm⁻¹) followed by a shoulder one (2625 cm⁻¹) is observed on the graphite sample, but only a relatively broad single peak (2670 cm⁻¹) appears in the spectra of **FLG-P** hybrids. The observations manifest once again that the exfoliated graphitic materials are few-layer graphene.[58]
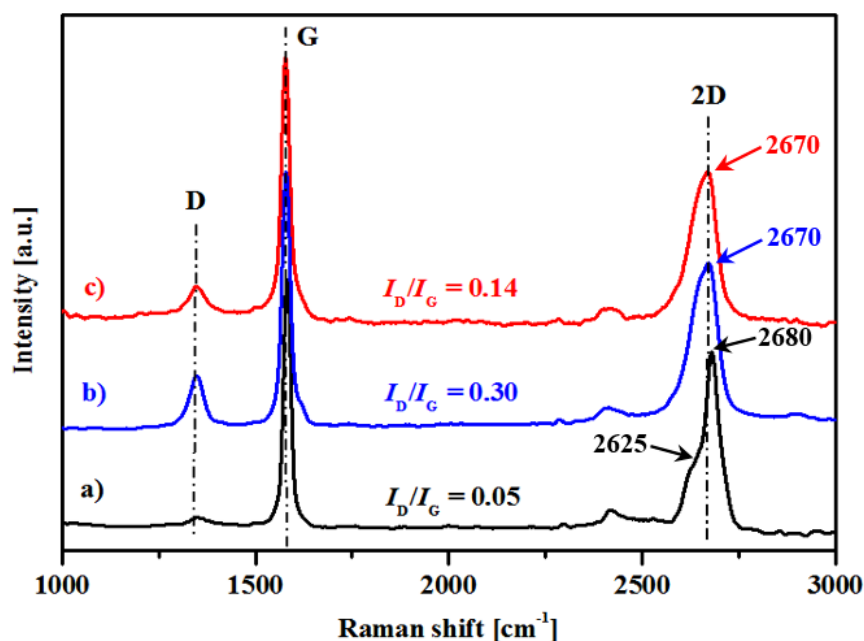
13

FIGURE 9 Raman spectra of a) graphite, b) **FLG-P-80**hybrid, and c) **FLG-P-20** hybrid.

Although polymer molecules residing on the FLG surface may be unwanted for some uses, they are really helpful for preparation of the flexible FLG films. Figure 10a shows a typical one prepared by vacuum filtration of aqueous dispersion of **FLG-P-80** hybrid (0.5 mg mL^{-1}) over a 25 nm hydrophilic membrane followed by drying in an oven at 70 °C. AFM analysis (Figure 10b) reveals that FLG sheets involved in the film are aligned parallel to the film plane. The obtained free-standing film (47 mm-diameter and 28 μm-thick) is robust and can be bent to an angle of ˜90° without breaking (Figure 10c). Even after 100 bendings, no cracks or delamination are observed by naked eyes. In microscopic scale, no discernible morphological changes occur before and after bending tests; average surface roughness only slightly increases from 151 to 160 nm (Figure 10d). As a sharp contrast, the film prepared from shear-exfoliated FLG in NMP or aqueous solution of SDBS breaks under the same bending condition. The toughening effect of VIB-*co*-VI-*co*-Py on FLG film is thus demonstrated. Moreover, the as-prepared film shows an electrical conductivity of 9.3 $\times$ 10^3 S m^{-1}. After annealing at 200°C for 10 h in N$_2$, it further increases to 4.0 $\times$ 10^4 S m^{-1} with no obvious weakening in bending tolerance. The combination of good toughness and excellent electrical conductivity in a single material system makes FLG films developed here very promising find some important applications, such as flexible and portable electronic devices.[59]
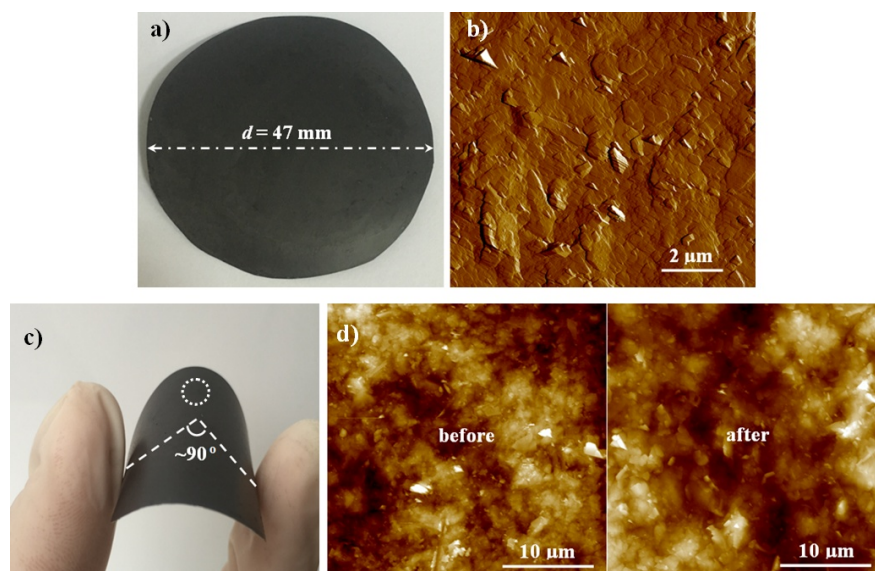
14

FIGURE 10 a) Photograph of a free-standing FLG film, b) AFM phase image of FLG film, c) photograph of FLG film bended to an angle of ˜90°, and d) AFM height images of circled area in c) before and after 100 times bending.

Plenty of affordable, high-quality, yet water-soluble graphene material is highly desirable for many applications, *e.g.* hydrophilic polymer composites.[17] The FLG-P hybrids nicely meet these requirements and were tested for preparation of polymer composite hydrogels. Figure 11a shows a typical PDMAA/FLG hydrogel synthesized by free-radical polymerization of DMAA in the presence of **FLG-P-80**hybrid. By comparing the weights of hydrogel and its fully dried sample, the water content is determined as 83 wt%. This hydrogel is mechanically tough and flexible. After compressing and then releasing the finger, it can promptly restore its shape and size (Figure 11a). The tensile testing shows that strength, modulus, and elongation at break reach 94 ± 6 kPa, 32 ± 1 kPa, and $288 \pm 21\%$, respectively, corresponding to 225%, 7%, and 202% increments relative to PDMAA hydrogel (Figure 11b). Moreover, this hydrogel is conductive with 1.1×10^{-3} S cm^{-1} of conductivity, compared with 7.5×10^{-8} S cm^{-1} for PDMAA hydrogel. This makes it a potential candidate material sustaining the tissue growth, and therein usually lies the demand on electrical stimulation.[60]
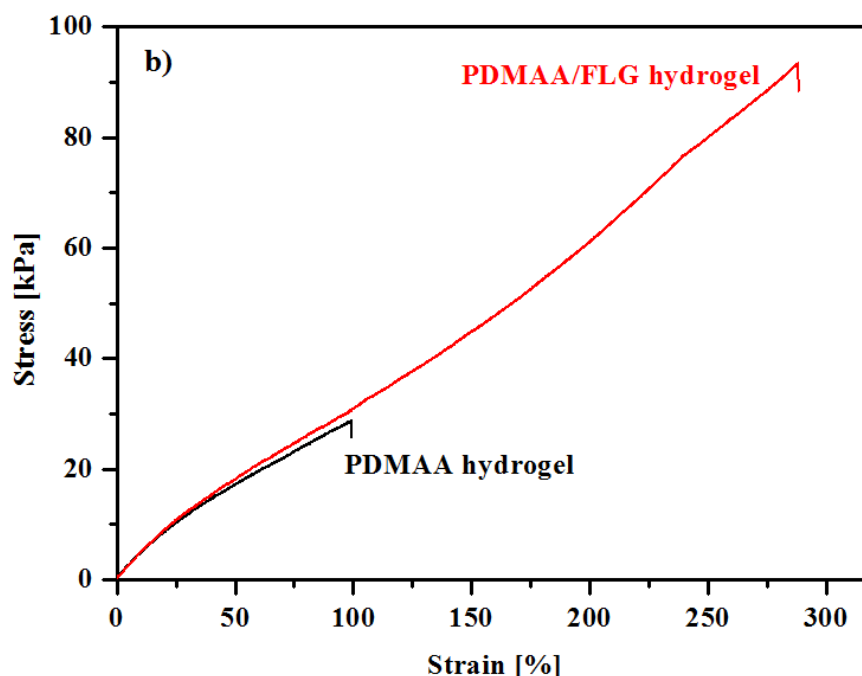

15
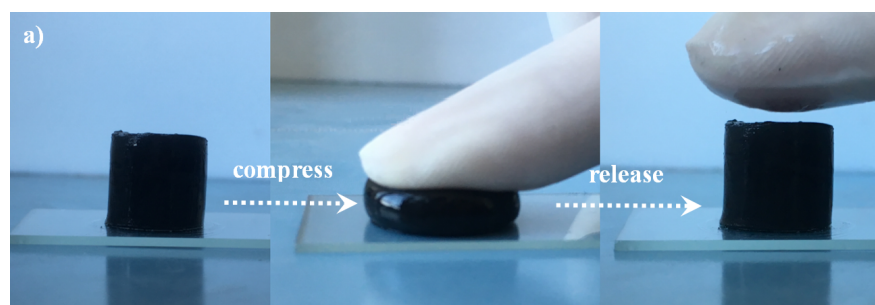
FIGURE 11 a) Photograph of a PDMAA/FLG hydrogel, and b) typical tensile stress-strain curves of PDMAA and PDMAA/FLG hydrogels.

CONCLUSIONS

With VIB-*co*-VI-*co*-Py serving as a water-soluble polymer stabilizer, the high-shear mixing of graphite in aqueous liquid was demonstrated to be a facile, green, and low-cost method for efficient production of FLG. In particular, $\mathbf{P_R/V}$ of FLG reaches as high as 0.17 g L^{-1} h^{-1}, significantly superior to those (1.6×10^{-3} - 8.3 x 10^{-2} g L^{-1} h^{-1}) realized by LPE with [?]5.0 L of aqueous liquid. It is ascribed to the combined contributions of excellent dispersing/stabilizing ability of VIB-*co*-VI-*co*-Py on FLG, little formation of large-sized micelles at high $C_\mathbf{P}$ (>3.0 mg mL^{-1}) under high-shear mixing, and little effect of $C_\mathbf{G,i}$ on shear force transmission. The harvested FLG shows high quality (few basal defects) and excellent electrical conductivity (up to 4.0 x 10^4 S m^{-1}), allowing for preparation of the flexible and conductive FLG films as a potential alternative to brittle ITO films. Furthermore, the FLG material exhibits a favorable redispersibility in water with $C_\mathbf{G}$ as high as 3.87 mg mL^{-1}. These merits together with low stabilizer content (down to 6.8 wt%) render the shear-exfoliated FLG very useful in various applications from polymer composites to electronics, especially those where FLG has to interface aqueous environment and/or only a small amount of stabilizer is allowed. Therefore, this work represents a meaningful attempt to forward the practical applications of graphene. In that direction, it is highly desirable for high-quality graphene or FLG to be mass produced in an economical and eco-friendly way.

ACKNOWLEDGEMENTS

ORCID

Yehai Yanhttps://orcid.org/0000-0002-3235-4247

Jian Cuihttps://orcid.org/0000-0001-7302-6402

REFERENCES

1. Deng B, Liu ZF, Peng HL. Toward mass production of CVD graphene films.*Adv Mater.* 2019;31:1800996.
2. Kong W, Kum H, Bae SH, Shim J, Kim H, Kong LP, Meng Y, Wang KJ, Kim C, Kim J. Path towards graphene commercialization from lab to market.*Nat Nanotechnol.* 2019;14: 927-938.
3. Yi M, Shen Z. A review on mechanical exfoliation for the scalable production of graphene. *J Mater Chem A* . 2015;3:11700-11715.
4. Stafford J, Patapas A, Uzo N, Matar OK, Petit C. Towards scale-up of graphene production via nonoxidizing liquid exfoliation methods.*AIChE J.* 2018;64:3246-3276.
5. Ciesielskia A, Samori P. Graphene via sonication assisted liquid-phase exfoliation. *Chem Soc Rev* . 2014;43:381-398.
6. Zocharia R, Ulbricht H, Hertel T. Interlayer cohesive energy of graphite from thermal desorption of polyaromatic hydrocarbons.*Phys Rev B* . 2004;69:155406.
7. Paton KR, Varrla E, Backes C, Smith R, Khan U, O'Neill A, Boland C, Lotya M, Istrate OM, King P, Higgins T, Barwich S, May P, Puczkarski P, Ahmed I, Moebius M, Pettersson H, Long E, Coelho J, O'Brien SE, McGuire EK, Sanchez BM, Duesberg GS, McEvoy N, Pennycook TJ, Downing C, Crossley A, Nicolosi V, Coleman JN. Scalable production of large quantities of defect-free few-layer graphene by shear exfoliation in liquids. *Nat Mater.* 2014;13:624-630.
8. Hernandez Y, Nicolosi V, Lotya M, Blighe FM, Sun Z, De S, McGovern IT, Holland B, Byrne M, Gun'Ko YK, Boland J, Niraj P, Duesberg G, Krishnamurti S, Goodhue R, Hutchison J, Scardaci V, Ferrari AC, Coleman JN. High-yield production of graphene by liquid-phase exfoliation of graphite. *Nat Nanotechnol.* 2008;3:563-568.
9. Khan U, O'Neill A, Lotya M, De S, Coleman JN. High-concentration solvent exfoliation of graphene. *Small* . 2010;6:864-871.
10. Bracamonte MV, Lacconi GI, Urreta SE, Foa Torres LEF. On the nature of defects in liquid-phase exfoliated graphene. *J Phys Chem C* . 2014;118:15455-15459.
11. Wahid MH, Eroglu E, Chen X, Smith SM, Raston CL. Functional multi-layer graphene- algae hybrid material formed using vortex fluidics. *Green Chem* . 2013;15:650-655.
12. Arao Y, Mori F, Kubouchi M. Efficient solvent systems for improving production of few- layer graphene in liquid phase exfoliation.*Carbon* . 2017;118:18-24.
13. Pattammattel A, Kumar CV. Kitchen chemistry 101: multigram production of high quality bi-ographene in a blender with edible proteins.*Adv Funct Mater.* 2015;25:7088-7098.
14. Gai Y, Wang W, Xiao D, Tan HJ, Lin MY, Zhao YP. Exfoliation of graphite into graphene by a rotor-stator in supercritical CO_2: experiment and simulation. *Ind Eng Chem Res.* 2018;57:8220-8229
15. Phiri J, Gane P, Maloney TC. High-concentration shear-exfoliated colloidal dispersion of surfactant-polymer-stabilized few-layer graphene sheets. *J Mater Sci.* 2017;52:8321-8337.
16. Liu L, Shen Z, Yi M, Zhang X, Ma S. A green, rapid and size-controlled production of high-quality graphene sheets by hydrodynamic forces.*RSC Adv.* 2014;4:36464-36470.
17. Hecht DS, Hu L, Irvin G. Emerging transparent electrodes based on thin films of carbon nan-otubes, graphene, and metallic nanostructures.*Adv Mater.* 2011;23:1482-1513.
18. Shi G, Araby S, Gibson CT, Meng Q, Zhu S, Ma J. Graphene platelets and their polymer composites: fabrication, structure, properties, and applications. *Adv Funct Mater.* 2018;28: 1706705.
19. Samoilov VM, Danilov EA, Nikolaeva AV, Yerpuleva GA, Trofimova NN, Abramchuk SS, Ponkratov KV. Formation of graphene aqueous suspensions using fluorinated surfactant- assisted ultrasonication

of pristine graphite. *Carbon.* 2015;84:38-46.

20. Large MJ, Ogilvie SP, Graf AA, Lynch PJ, O'Mara MA, Waters T, Jurewicz I, Salvage JP, Dalton AB. Large-scale surfactant exfoliation of graphene and conductivity-optimized graphite enabling wireless connectivity. *Adv Mater Technol.* 2020;5:2000284.

21. Lotya M, King PJ, Khan U, De S, Coleman JN. High-concentration, surfactant- stabilized graphene dispersions. *ACS Nano.*2010;4:3155-3162.

22. Viinikanoja A, Kauppila J, Damlin P, Makilad E, Leiro J, Aaritalo T, Lukkari J. Interactions between graphene sheets and ionic molecules used for the shear-assisted exfoliation of natural graphite.*Carbon.* 2014;68:195-209.

23. Parviz D, Das S, Tanvir Ahmed HS, Irin F, Bhattacharia S, Green MJ. Dispersions of non-covalently functionalized graphene with minimal stabilizer. *ACS Nano.* 2012;6:8857- 8867.

24. Lee DW, Kim T, Lee M. An amphiphilic pyrene sheet for selective functionalization of graphene. *Chem Commun.* 2011;47:8259-8261.

25. Cui J, Song Z, Xin L, Zhao S, Yan Y, Liu G. Exfoliation of graphite to few-layer graphene in aqueous media with vinylimidazole-based polymer as high-performance stabilizer. *Carbon* . 2016;99:249-260.

26. Shang JQ, Ding EY, Xue F, Zeng XR, Chen JW, Xu N, Zhang NC, Wei QS. High concentration of few-layer graphene and MoS2 nanosheets using carboxyl methyl cellulose as a high-performance stabilizer.*Micro & Nano Lett.* 2019;14:835-839.

27. Gravagnuolo AM, Morales-Narvaez E, Longobardi S, da Silva ET, Giardina P, Merkoci A. In situ production of biofunctionalized few-layer defect-free microsheets of graphene. *Adv Funct Mater.*2015;25:2771-2779.

28. Parab AD, Budi A, Slocik JM, Rao R, Naik RR, Walsh TR, Knecht MR. Molecular-level insights into biologically driven graphite exfoliation for the generation of graphene in aqueous media. *J Phys Chem C.*2020;124:2219-2228.

29. Carrasco PM, Montes S, Garcia I, Borghei M, Jiang H, Odriozola I, Cabanero G, Ruiz V. High-concentration aqueous dispersions of graphene produced by exfoliation of graphite using cellulose nanocrystals.*Carbon.* 2014;70:157-163.

30. Sun Z, Vivekananthan J, Guschin DA, Huang X, Kuznetsov V, Ebbinghaus P, Sarfraz A, Muhler M, Schuhmann W. High-concentration graphene dispersions with minimal stabilizer: a scaffold for enzyme immobilization for glucose oxidation. *Chem Eur J.* 2014; 20:5752-5761.

31. Joseph D, Seo S, Williams DR, Geckeler KE. Double-stranded DNA-graphene hybrid: Preparation and anti-proliferative activity.*ACS Appl Mater Interfaces.* 2014;6:3347-3356.

32. Liu Z, Liu J, Cui L, Wang R, Luo X, Barrow CJ, Yang W. Preparation of graphene/ polymer composites by direct exfoliation of graphite in functionalised block copolymer matrix. *Carbon* . 2013;51:148-155.

33. Fan J, Shi Z, Ge Y, Wang J, Wang Y, Yin J. Gum arabic assisted exfoliation and fabrication of Ag-graphene-based hybrids. *J Mater Chem.* 2012;22:13764-13772.

34. May P, Khan U, O'Neill A, Coleman JN. Approaching the theoretical limit for reinforcing polymers with graphene. *J Mater Chem.*2012;22:1278-1282.

35. Liu F, Choi JY, Seo TS. DNA mediated water-dispersible graphene fabrication and gold nanoparticle-graphene hybrid. *Chem Commun.*2010;46:2844-2846.

36. Bourlinos AB, Georgakilas V, Zboril R, Steriotis TA, Stubos AK, Trapalis C. Aqueous phase exfoliation of graphite in the presence of polyvinylpyrrolidone for the production of water-soluble graphenes. *Solid State Commun.* 2009;149:2172-2176.

37. Xu M, Zhang W, Yang Z, Yu F, Ma Y, Hu N, He D, Liang Q, Su Y, Zhang Y. One-pot liquid-phase exfoliation from graphite to graphene with carbon quantum dots. *Nanoscale* . 2015;7:10527-10534.

38. Alhassan SM, Qutubuddin S, Schiraldi DA. Graphene arrested in laponite-water colloidal glass. *Langmuir* . 2012;28:4009-4015.

39. Tung TT, Yoo J, Alotaibi FK, Nine MJ, Karunagaran R, Krebsz M, Nguyen GT, Tran DN, Feller JF, Losic D. Graphene oxide-assisted liquid phase exfoliation of graphite into graphene for highly conductive film and electromechanical sensors. *ACS Appl Mater Interfaces.* 2016;8:16521-16532.

40. Song Z, Dai J, Zhao S, Zhou Y, Su F, Cui J, Yan Y. Aqueous dispersion of pristine single- walled carbon

nanotubes prepared by using a vinylimidazole-based polymer dispersant. *RSC Adv.*2014;4:2327-2338.

41. Pozharskii AF, Soldatenkov AT, Katritzky AR. *Heterocycles in life and society: an introduction to heterocyclic chemistry, biochemistry, and applications* . John Wiley & Sons: Chichester; 2011.

42. Ferris CJ, in het Panhuis M. Conducting bio-materials based on gellan gum hydrogels. *Soft Matter* . 2009;5:3430-3437.

43. Wang H, Chen Z, Xin L, Cui J, Zhao S, Yan Y. Synthesis of pyrene-capped polystyrene by free radical polymerization and its application in direct exfoliation of graphite into graphene nanosheets. *J Polym Sci Part A: Polym Chem.* 2015;53:2175-2185.

44. Vigolo B, Penicaud A, Coulon C, Sauder C, Pailler R, Journet C, Bernier P, Poulin P. Macroscopic fibers and ribbons of oriented carbon nanotubes. *Science.* 2000;290:1331- 1334

45. Ayan-Varela M, Paredes JI, Guardia L, Villar-Rodil S, Munuera JM, Díaz-Gonzalez M, Fernandez-Sanchez C, Martínez-Alonso A, Tascon JMD. Achieving extremely concentrate aqueous dispersions of graphene flakes and catalytically efficient graphene-metal nanoparticle hybrids with flavin mononucleotide as a high-performance stabilizer. *ACS Appl Mater Interfaces* . 2015;7:10293-10307.

46. Lotya M, Hernandez Y, King PJ, Smith RJ, Nicolosi V, Karlsson LS, Blighe FM, De S, Wang ZM, McGovern IT, Duesberg GS, Coleman JN. Liquid phase production of graphene by exfoliation of graphite in surfactant/water solutions. *J Am Chem Soc* . 2009; 131:3611-3620.

47. Sun Z, Masa J, Liu Z, Schuhmann W, Muhler M. Highly concentrated aqueous dispersions of graphene exfoliated by sodium taurodeoxycholate: dispersion behavior and potential application as a catalyst support for the oxygen-reduction reaction. *Chem Eur J* . 2012;18: 6972-6978.

48. Shahil KM, Balandin AA. Graphene-multilayer graphene nanocomposites as highly efficient thermal interface materials. *Nano Lett* . 2012;12:861-867.

49. Texter J. A kinetic model for exfoliation kinetics of layered materials. *Angew Chem Int Ed* . 2015;54:10258-10262.

50. Holland FA, Chapman FS. *Liquid mixing and processing in stirred tanks* . Reinhold Publishing: New York; 1966.

51. Zeta potential – An introduction in 30 minutes*https://wwwmalverncom/en/support/ resource-center/technical-notes/TN101104ZetaPotentialIntroductionhtml.*

52. Park S, Ruoff RS. Chemical methods for the production of graphene.*Nat Nanotechnol* . 2009;4:217-224.

53. Nemes-Incze P, Osvath Z, Kamaras K, Biro LP. Anomalies in thickness measurements of graphene and few layer graphite crystals by tapping mode atomic force microscopy. *Carbon* . 2008;46:1435-1442.

54. Fasolino A, Los JH, Katsnelson MI. Intrinsic ripples in graphene.*Nat Mater.* 2007;6:858- 861.

55. Meyer JC, Geim AK, Katsnelson MI, Novoselov KS, Booth TJ, Roth S. The structure of suspended graphene sheets. *Nature* . 2007;446:60-63.

56. Tung VC, Allen MJ, Yang Y, Kaner RB. High-throughput solution processing of large- scale graphene. *Nat Nanotechnol* . 2009;4:25-29.

57. Mohanty N, Nagaraja A, Armesto J, Berry V. High-throughput, ultrafast synthesis of solution-dispersed graphene via a facile hydride chemistry. *Small* . 2010;6:226-231.

58. Ferrari AC, Meyer JC, Scardaci V, Casiraghi C, Lazzeri M, Mauri F, Piscanec S, Jiang D, Novoselov KS, Roth S, Geim AK. Raman spectrum of graphene and graphene layers. *Phys Rev Lett* . 2006;97:187401.

59. Wang C, Xia K, Wang H, Liang X, Yin Z, Zhang Y. Advanced carbon for flexible and wearable electronics. *Adv Mater* . 2019;31:1801072.

60. Ahadian S, Ramón-Azcón J, Ostrovidov S, Camci-Unal G, Kaji H, Ino K, Shiku H, Khademhosseini A, Matsue T. A contactless electrical stimulator: application to fabricate functional skeletal muscle tissue. *Biomed Microdev.* 2013;15:109-115.

SUPPORTING INFORMATION

Additional supporting information may be found online in the Supporting Information section at the end of this article.